Electronic Supplementary Material (ESI) for Journal of Materials Chemistry A.

Supporting Information

Ionic Liquid Modified SnO_2 Nanocrystals as the Robust Electron Transporting Layer for Efficient Planar Perovskite Solar Cells

Chun Huang[a,b], Peng Lin[a], Nianqing Fu[c], Kaiwen Sun[f], Mao Ye[d], Chang Liu[d], Xianyong Zhou[d], Longlong Shu[e], Xiaojing Hao[f], Baomin Xu[d], Xierong Zeng[a], Yu Wang[e], and Shanming Ke[a,e*]*

[a]College of Materials Science and Engineering, Shenzhen University, Shenzhen 518060, P. R. China

[b]College of Optoelectronic Engineering and Key Laboratory of Optoelectronic Devices and Systems of Ministry of Education and Guangdong Province, Shenzhen University, Shenzhen 518060, P. R. China

[c]School of Materials Science and Engineering, South China University of Technology, Guangzhou 510640, P. R. China

E-mail: msnqfu@scut.edu.cn

[d]Department of Materials Science and Engineering, Southern University of Science and Technology, Shenzhen 518060, P. R. China

[e]School of Materials Science and Engineering, Nanchang University, Nanchang 330031, Jiangxi, P. R. China

E-mail: keshanming@gmail.com

[f]School of Photovoltaic and Renewable Energy Engineering, University of New South Wales, Sydney 2052, New South Wales, Australia

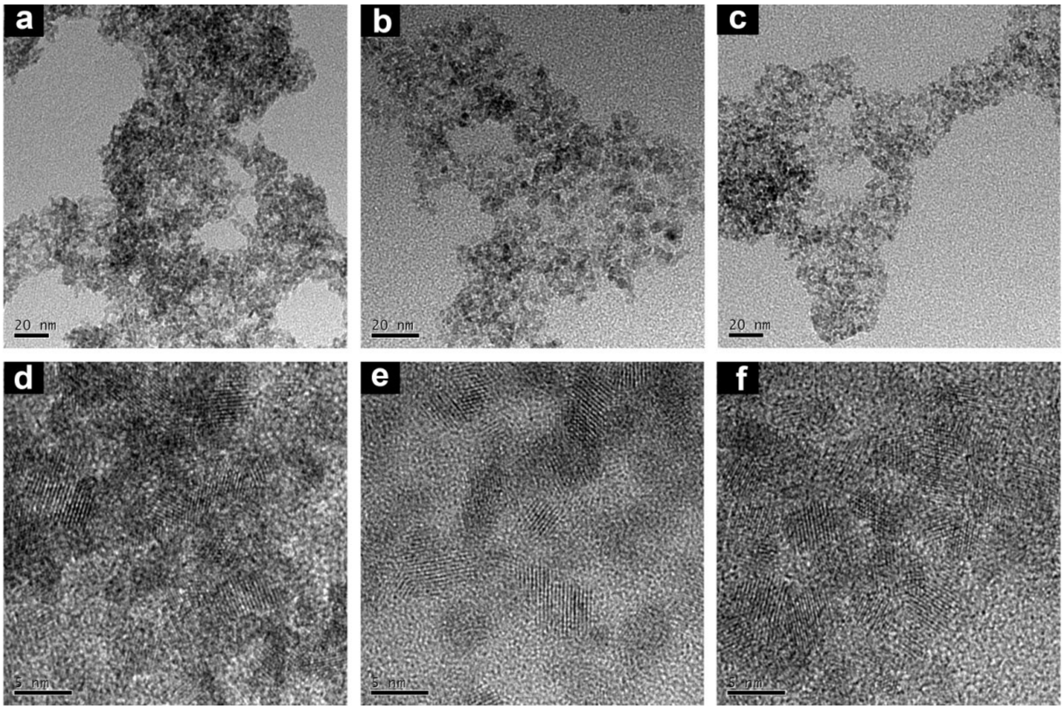

Fig. S1. TEM images of (a) n-SnO_2 nanoparticles, (b) fresh TMAH-modified SnO_2 nanoparticles and (c) TMAH-modified SnO_2 store for 12 hs. (d), (e) and (f) are the corresponding HRTEM images of (a), (b) and (c), respectively.

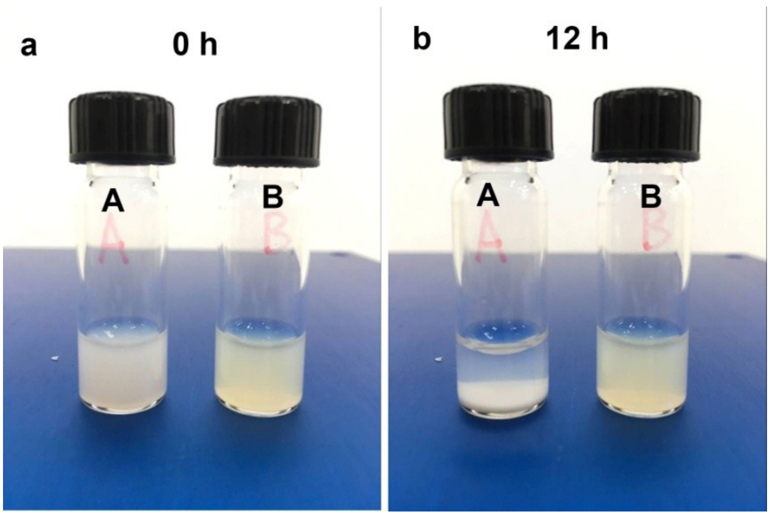

Fig. S2. Dispersion of SnO_2 nanoparticles at 0 h and 12 h. A without TMAH; B with TMAH modification.

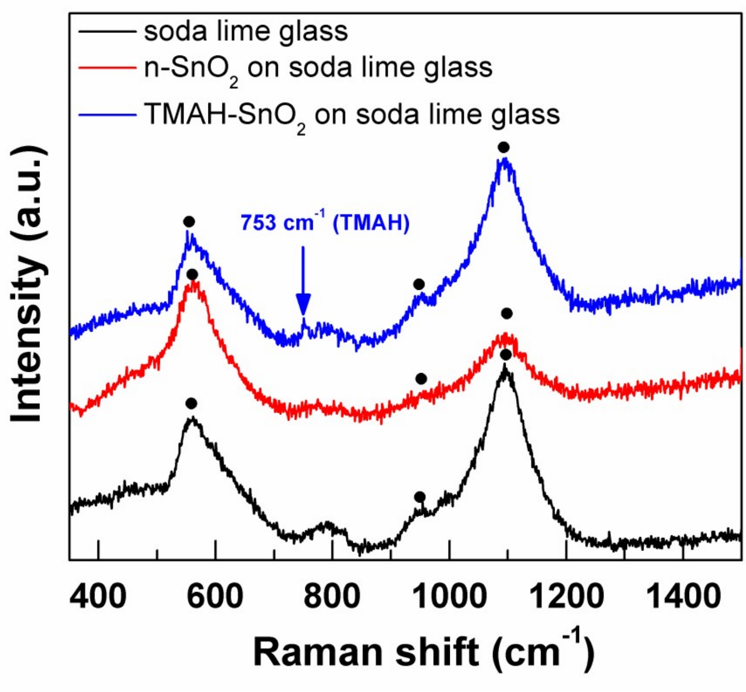

Fig. S3. Raman spectra of soda lime glass substrate (black line), n-SnO_2 on soda lime glass (red line), and TMAH-SnO_2 on soda lime glass. The dark dot indicate the Raman shift for soda lime glass. Peak located at about 753 cm^{-1} is a signal of TMAH.

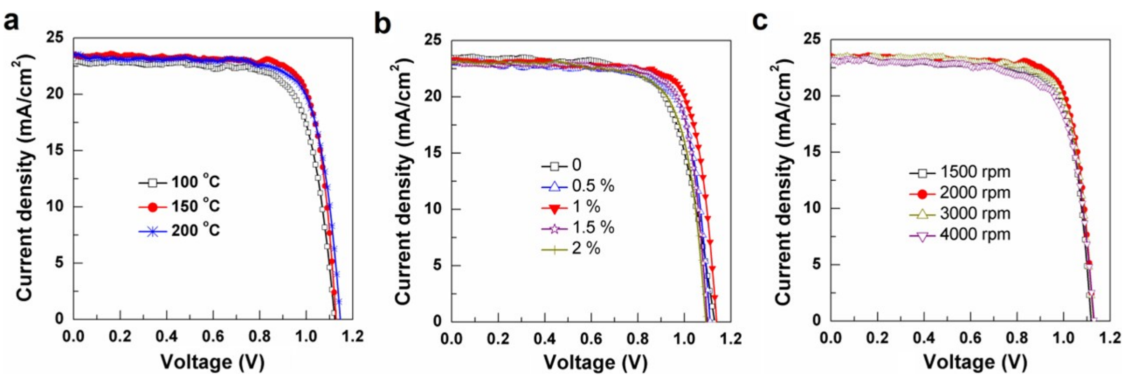

Fig. S4. Optimization of the ETL deposition process. The (a) annealing temperature, (b) TMAH concentration, and (c) spin-coating speed dependent performance of the PSCs. It can be learned that 1 % concentration of TMAH, 2000 rpm of spin coating rate, and 150 °C of annealing temperature is optimized for efficient devices.

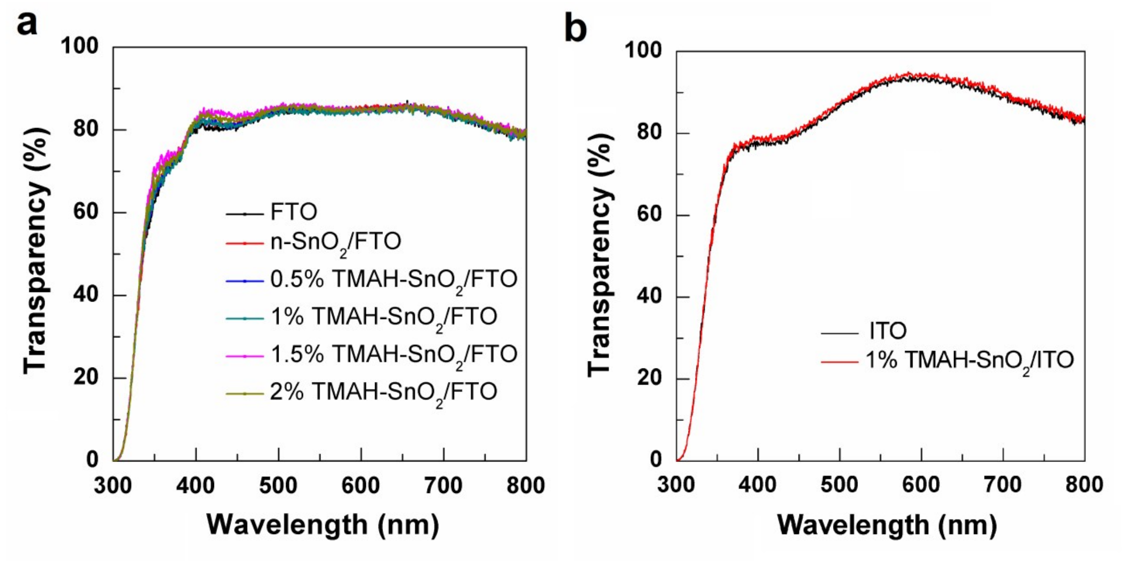

Fig. S5. Optical transmittance of the (a) bare FTO and SnO_2 coated FTO substrates, and (b) bare ITO and SnO_2 coated ITO substrates.

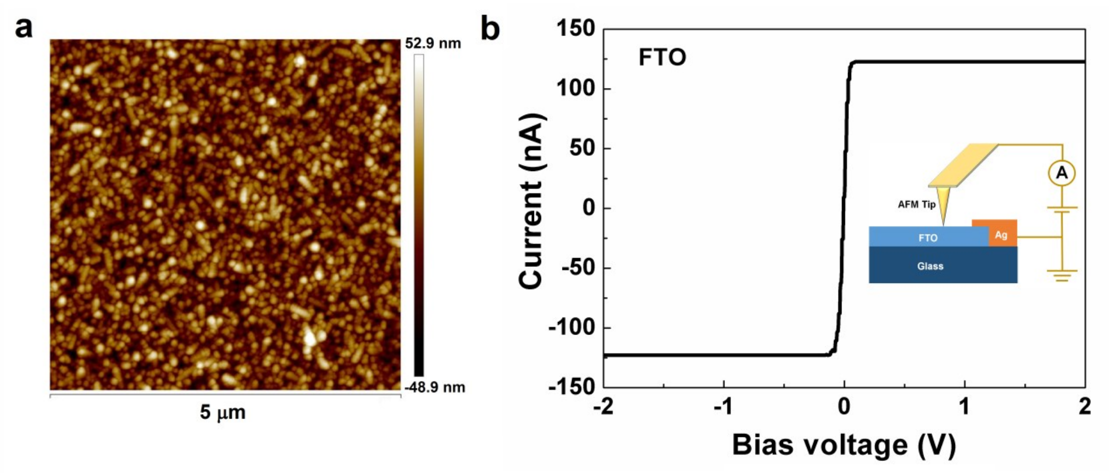

Fig. S6. (a) Mophology and (b) *I-V* curve of a FTO substrate from c-AFM measurement, showing ohm contact between the tip and the FTO electrode.

Table S1. Summary of hall measurements on SnO_2 films

Materials	Sheet resistance (MΩ)	Resistivity (ohm·cm)	Mobility ($cm^2 \cdot v^{-1} \cdot s^{-1}$)	Carrier concentration (cm^{-3})
n-SnO_2	214	1.81×10^2	3.02	1.14×10^{16}
TMAH-SnO_2	58	1.20×10^2	4.16	1.24×10^{16}

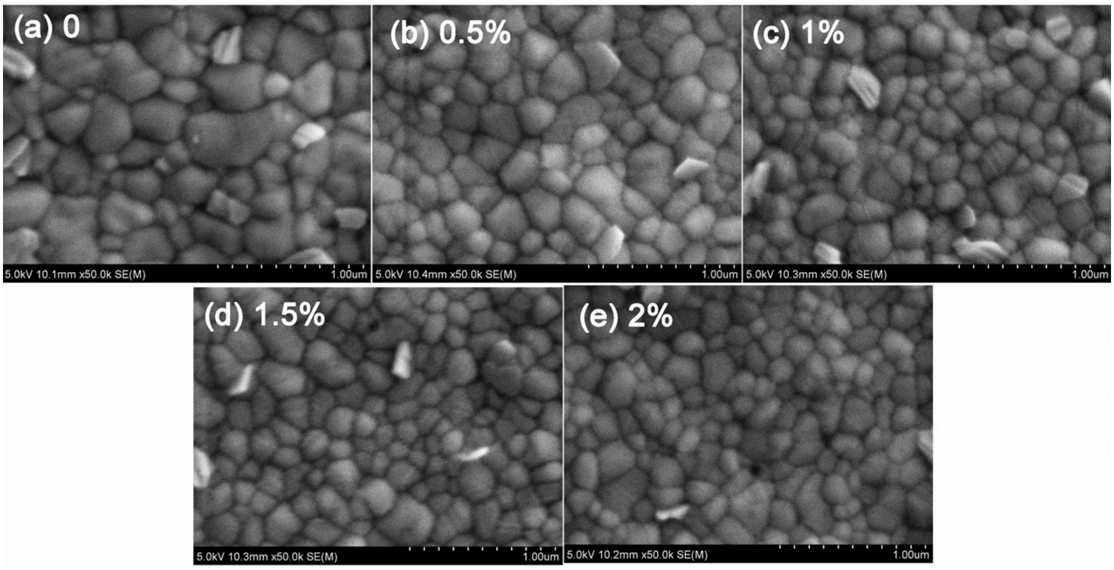

Fig. S7. Surface SEM images for perovskite deposited on (a) n-SnO_2, (b) 0.5% TMAH-SnO_2, (c) 1% TMAH-SnO_2, (d) 1.5% TMAH-SnO_2 and (e) 2% TMAH-SnO_2, respectively.

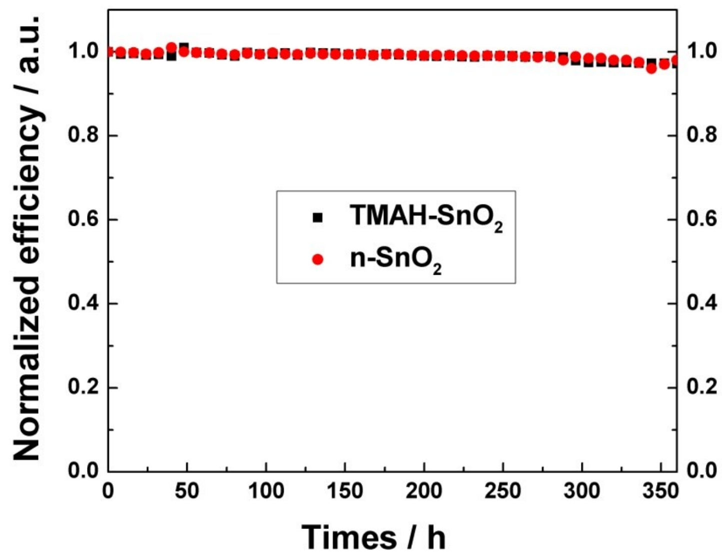

Fig. S8. Stability tests for n-SnO_2 based and TMAH-SnO_2 based devices sealed with resin. Devices were stored in desiccator under relative humidity of about 15%.

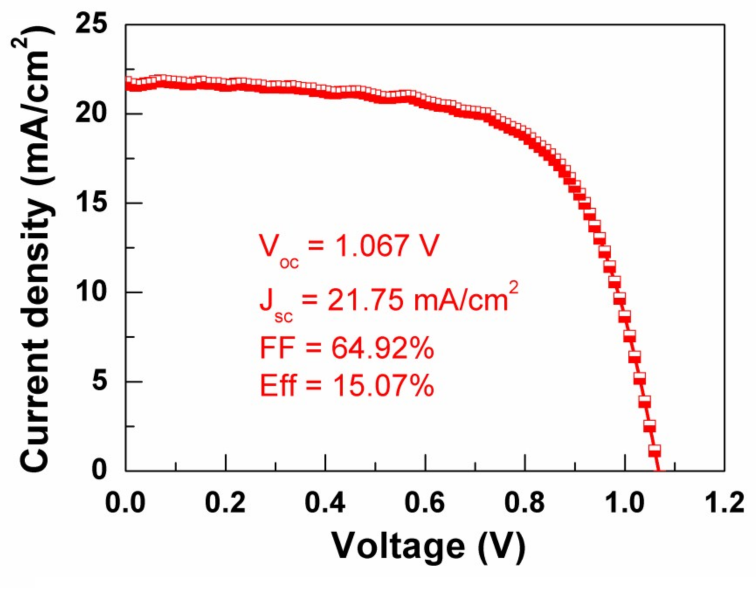

Fig. S9. *J-V* curve of a flexible TMAH-SnO_2 based device constructed on ITO/PEN substrate, showing an efficiency of about 15.07%.